A Direct Simulation-Based Study of Radiance in a Dynamic Ocean

Dick K.P. Yue
Center for Ocean Engineering
Massachusetts Institute of Technology
Room 5-321, 77 Massachusetts Ave, Cambridge, MA 02139
phone: (617) 253-6823 fax: (617) 258-9389 email: yue@mit.edu

Yuming Liu
Center for Ocean Engineering
Massachusetts Institute of Technology
Room 5-326C, 77 Massachusetts Ave, Cambridge, MA 02139
phone: (617) 252-1647 fax: (617) 258-9389 email: yuming@mit.edu

Award Number: N00014-06-1-0027
http://www.mit.edu/~vfrl/

LONG-TERM GOALS

The ultimate goal is to develop direct simulation/physics-based forward and inverse capabilities for radiance prediction in a dynamic ocean environment. The simulation-based model will include and integrate all of the relevant dynamical processes in the upper ocean surface boundary layer into a physics-based computational prediction capability for the time-dependent radiative transport.

OBJECTIVES

To include and integrate relevant dynamical processes in the upper ocean surface boundary layer (SBL) into a physics-based computational prediction and inverse capability for the time-dependent radiative transport:

- Develop direct simulation of upper ocean hydrodynamic processes and forward prediction of radiative transfer
- Obtain understanding, modeling and parameterizations of dependencies of oceanic radiance on the surface wave environment
- Provide guidance for field measurements and obtain cross validations and calibrations with direct simulations and modeling
- Provide a framework for inverse modeling and reconstruction of ocean surface and above water features based on sensed underwater radiance data

To reach these objectives, we had and would continue to have a close collaboration with Professor Lian Shen of the Johns Hopkins University (JHU) on the modeling of free surface turbulence roughness.

APPROACH

A simulation approach, based on direct physics-based simulations and modeling, is developed and applied to solve the problem of ocean radiance transport (RT) in a dynamic ocean SBL environment that includes nonlinear capillary-gravity waves (CGW), free-surface turbulence (FST) roughness, wave breaking, and bubble generation and transport. The radiative transport is governed by Snell's law and Fresnel transmission at the water surface, and absorption and multiple scattering in the water underneath. The complex dynamic processes of the ocean SBL, the nonlinear CGW interactions, the development and transport of FST, and the generation and transport of bubbles are modeled using physics-based computations. The modeling of these hydrodynamic processes is coupled with the computation of radiative transport.

(1) Radiative Transfer in CGW and FST: Monte Carlo simulation of radiance transfer (RT) (e.g. Walker 1994) is developed with the free surface deformation obtained from direct CGW and FST computations. The effects of absorption and multiple scattering on RT are included. Bubble scattering effects are also considered based on bubble distribution and transport and Mie theory.

(2) Nonlinear CGW: An efficient phase-resolved computational approach based on Euler equations is used to compute spatial and temporal nonlinear evolution of capillary and gravity waves. This computational tool builds on an efficient high-order spectral method that we developed for direct simulations of nonlinear gravity wavefield evolution. Nonlinear gravity-gravity and gravity-capillary wave interactions in a broadband wave spectrum are accounted for up to an arbitrary order in the wave steepness. With high computational efficiency, this approach enables phase-resolved simulations of large-scale nonlinear CGW.

(3) Steep and Breaking Waves: A Navier-Stokes equations solver for fully coupled air-wave interactions with a level-set method for free surface tracking is employed to compute the details of free surface signature and dissipation due to steep and breaking waves.

(4) FST-Wave Interactions: Navier-Stokes equations based DNS is employed to resolve all eddies in free surface turbulence. LES and LWS are used to compute large eddy and large wave components explicitly, with effects from small-scale motions being represented by subgrid-scale (SGS) models. Fully nonlinear viscous free-surface boundary conditions are imposed. Effects of surfactants are captured through the Plateau-Marangoni-Gibbs effect with surfactant transport directly simulated.

(5) Bubble Transport in CGW and FST: Direct simulation is developed to compute bubble motion in CGW and FST environment. Both Lagrangian and Eulerian approaches are used to trace bubble trajectories. Bubble motion is subject to forces due to added mass, buoyancy, drag, lift, and fluid stress gradients arising from the continuous-phase acceleration. Bubble source is determined based on experimental measurements and/or existing data.

Yue and Liu at MIT will be responsible for the study of (1), (2) and (3) as well as integration of (4) and (5) into the simulation capability while Shen at JHU will be responsible for the study and development of (4) and (5).

WORK COMPLETED

- ***Development of nonlinear CGW simulation capability***: Continued the development and verification of a direct simulation capability for nonlinear CGW evolution by extending the

high-order spectral method for gravity waves to general broadband nonlinear wave interactions involving swell, seas, and capillary waves. The focus was on the inclusion of capillary wave dynamics, long-short wave interactions, wave breaking dissipation, dissipation due to free surface turbulence and energy input by wind.

- ***Development of 3D Monte Carlo RT simulation for atmosphere-ocean system***: We developed a three-dimensional coupled atmosphere-ocean Monte Carlo radiative transfer (RT) simulation capability for both polarized and unpolarized lights. The RT simulation is time independent, but accounts for the effects of unsteady three-dimensional ocean surface. Multiple refractions at ocean surface, total internal reflection, all orders of multiple scattering, and scattering and absorption of both water molecules and marine aerosols are all considered. Various techniques including the use of biased sampling algorithms and parallelization of the code (with MPI) were employed to speed up the program for practical applications.

- ***Application of RT simulations in CGW and FST environments***:
  - Continued to validate the 3D polarized Monte Carlo RT codes for the atmosphere-ocean system by comparisons to available experimental data and other model predictions
  - Understood the key characteristics of irradiance and polarization distributions under regular and irregular waves
  - Studied the effect of surface wave nonlinearity upon the polarization distribution
  - Investigated the dependence of underwater irradiance variance on wave steepness
  - Investigated the characteristics of underwater imaging of above-water sources
  -
  - Performed 3D Monte Carlo RT simulations for variable density/refractive index and application to ocean turbulence

RESULTS

We continued to systematically validate the RT simulations by making direct comparisons with theories, existing numerical model prediction, and available experimental measurements. The developed RT model was used to investigate the characteristics of polarization distribution and underwater irradiance in various ocean surface environments. Of particular interest are the distinct features of polarization distribution under regular and irregular waves as well as the wave steepness effect upon the distribution of underwater irradiance along the depth.

Validation of the 3D Monte Carlo RT simulations: Figure 1 shows a sample validation result of the comparison between the present 3D Monte Carlo RT simulation and the prediction by the multi-component approximation method. Excellent agreement between them is obtained for the averaged degree of polarization distribution received at the optical depth $cz = 0.01$ under the water surface. The two cases shown are for incident sun with zenith angles $\theta_s = 0°$ and 60°. For both cases, incident sun has an azimuth angle of $\varphi_s = 0°$ and the water surface is flat. The other physical and computational parameters used in the computation are: atmosphere optical thickness $\tau_a = 0.15$, ocean optical thickness $\tau_o = 1.0$, H-G phase function $g = 0.75$, number of photons $M = 10^8$, and number of grids in the horizontal plane $N = 128^2$.

Effects of ocean surface upon underwater radiance and polarization distributions: To understand the characteristics of underwater radiance and polarization distributions, we performed the 3D Monte

Carlo RT simulations under various incident sun and surface wave conditions. Figure 2 presents a sample simulation result of the underwater radiance and polarization distributions under the flat surface, regular waves and irregular waves for incident sun with zenith angle θ_s= 30° and azimuth angle φ_s=135° The receiver is located at the optical depth cz = 1.0 under the mean ocean surface. The regular waves have a wave steepness kA = 0.40 while the irregular waves, given by a JONSWAP wave spectrum, have a peak wave steepness k_pA_p = 0.40. In the simulations, we use atmosphere optical thickness τ_a= 0.15, ocean optical thickness τ_o = 10, absorption coefficient a = 0.179 m^{-1}, scattering coefficient b = 0.219 m^{-1}, H-G phase function g = 0.924, and single scattering albedo ω_0 =0.99. Depending on the ocean surface roughness, underwater radiance and polarization distributions exhibit distinctive patterns. In the presence of irregular waves, due to the diffuse effect of short waves, the degree of polarization in the Sneil's cone (Θ<48°) is much larger than that in the case of regular waves or flat surface.

Ocean wave steepness effects upon underwater irradiance distribution: Figure 3 shows the distribution of the underwater irradiance variance along the optical depth under irregular waves with three peak wave steepness k_pA_p= 0.3, 0.2, and 0.1, obtained using the 3D Monte Carlo RT simulations. The irradiance variance is defined by

$$\sigma_E^2(z) \equiv \frac{< (E(x,z) - < E > (z))^2 >}{< E >^2 (z)}$$

where < > represents the average over the horizontal plane, *x* and *y*, and E is irradiance. In the simulations, we use (θ_s, φ_s) = (0, 0) (i.e. black sky), a = 0.179 m^{-1}, b = 0.219 m^{-1}, and H-G phase function g = 0.924. The irregular ocean waves are generated based on the linear and nonlinear wave theories with a JONSWAP wave spectrum. For a given wave steepness, irradiance variance for nonlinear waves is consistently lower than that for linear waves. After certain optical depth, irradiance variances under both linear and nonlinear waves reach the same asymptotic. Significantly, irradiance variance is seen to grow with the wave steepness. The difference in the variances obtained with linear and nonlinear waves increases monotonically with the wave steepness.

IMPACT/APPLICATIONS

The capability of accurate prediction of the irradiance transfer across ocean surface and in the water may enable the development of a novel approach for accurate measurements of complex ocean boundary layer processes and reliable detection of structures/objects on or above ocean surface based on sensed underwater irradiance data.

PUBLICATION

1. Kofiani, K. N. "A New Numerical Method for the Problem of Nonlinear Long-Short Wave Interactions", MS thesis, Massachusetts Institute of Technology, August, 2009.

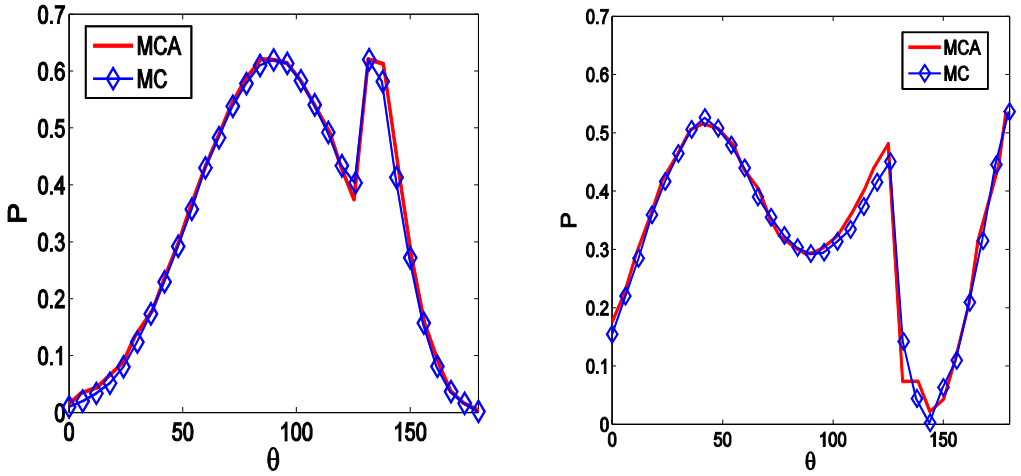

Figure 1: Comparisons of the present Monte Carlo RT simulation (blue line with symbols) with the prediction by the Multi-Component Approximation method (red line). The plotted is the averaged degree of polarization as a function of polar angle θ observed at optical depth cz = 0.01, for incident sun with (a) zenith angle θ_s= 0° and azimuth angle φ_s=0°; and (b) θ_s= 60° and φ_s=0°.

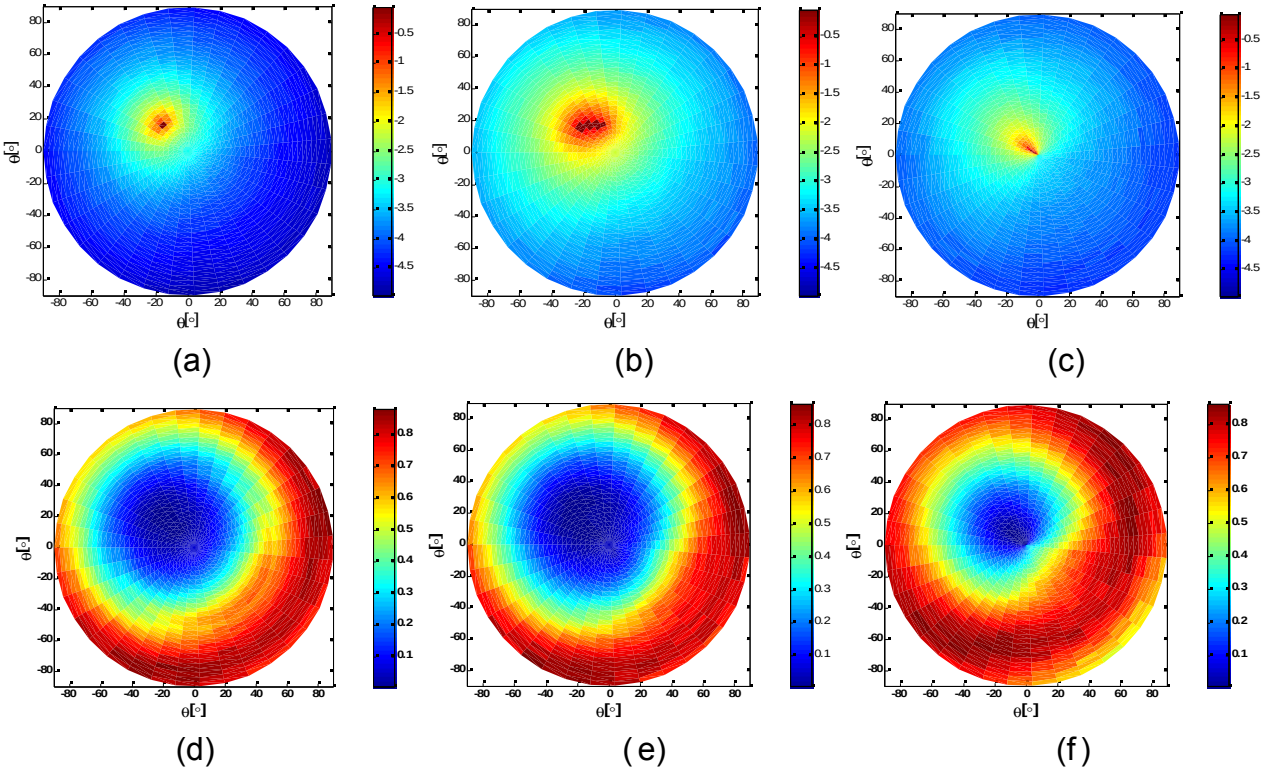

Figure 2. Vector radiance I(θ) (top: a, b, c) and averaged degree of polarization P(θ) (bottom: d, e, f) under flat surface (left: a, d), regular waves (middle: b, e) and irregular waves (right: c, f), received at optical depth cz = 1.0 under the mean ocean surface. Incident sun has zenith angle θ_s= 30° and azimuth angle φ_s=135°.

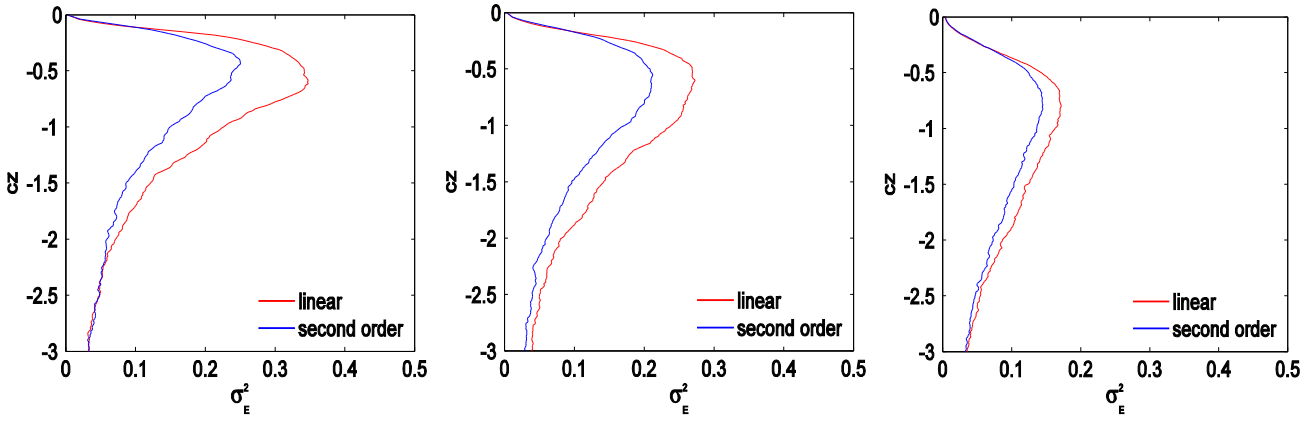

(a) (b) (c)

Figure 3. Dependence of underwater irradiance variance (σ^2) at various optical depth (cz) on surface wave steepness: (a) wave steepness k_pA_p = 0.30, (b) k_pA_p = 0.20, and (c) k_pA_p = 0.10. The results are obtained with the ocean surface wave given by the linear wave theory (red line) and the nonlinear wave theory including the second-order wave effects (blue line).